Atmospherically Resistant Vegetation Index (ARVI) for EOS-MODIS

Yoram J. Kaufman and Didier Tanré

Abstract—**Atmospherically resistant vegetation index (ARVI) is proposed and developed to be used for remote sensing of vegetation from the Earth Observing System (EOS) MODIS sensor. The same index can be used for remote sensing from Landsat TM, and the EOS-HIRIS sensor. The index takes advantage of the presence of the blue channel (0.47±0.01 μm) in the MODIS sensor, in addition to the red (0.66±0.025 μm) and the near IR (0.865±0.02 μm) channels that compose the present normalized difference vegetation index (NDVI). The resistance of the ARVI to atmospheric effects (in comparison to the NDVI) is accomplished by a self-correction process for the atmospheric effect on the red channel, using the difference in the radiance between the blue and the red channels to correct the radiance in the red channel. Simulations using radiative transfer computations on arithmetic and natural surface spectra, for various atmospheric conditions, show that ARVI has a similar dynamic range to the NDVI, but is, on average, *four times less sensitive* to atmospheric effects than the NDVI. The improvement is much better for vegetated surfaces than for soils. It is much better for moderate to small size aerosol particles (e.g., continental, urban, or smoke aerosol) than for large particle size (e.g., maritime aerosol or dust). Due to a fortunate coincidence, the same optimal value of the parameter γ that defines the weighting of the blue band radiance in the ARVI definition, is found for vegetated areas with small to moderate aerosol particle size (e.g., anthropogenic aerosol and smoke) and for arid regions with large particle size (e.g., dust). Therefore, a single combination of the blue and the red channels in the ARVI may be used in all or most remote sensing applications. Due to the excellent atmospheric resistance of the ARVI, it is expected that remote sensing from MODIS of the vegetation index over most land surfaces will include molecular and ozone correction with no further need for aerosol correction, except for dust conditions, like in the Sahel.**

I. Introduction

The Normalized Difference Vegetation Index (NDVI) derived from meteorological satellite data is used to detect changes in global vegetation [1], [2]. It is computed from the difference between the near-IR, L_{NIR}, and the red, L_{red}, radiances reflected from the surface and transmitted through the atmosphere:

$$NDVI = (L_{NIR} - L_{red})/(L_{NIR} + L_{red}). \quad (1)$$

This difference is sensitive to the presence of vegetation, since green vegetation usually decreases the signal in the red due to chlorophyl absorption and increases the signal in the near IR [3]. In Fig. 1, typical spectra of vegetation and soils are plotted (based on data from Bowker *et al.* [4]), showing the sensitivity of the red and near-IR reflectances to vegetation. The NDVI was shown to be related to canopy photosynthesis [5], and NDVI integrated throughout the growing season is sensitive to primary productivity [6], to the rainfall in semiarid regions [7], and to seasonal and latitudinal variations of the atmospheric CO_2 concentration [8]. As such it was applied to regional [9]–[11] and global vegetation problems.

The success of the NDVI to monitor vegetation variations on a large scale, despite the degradation of the AVHRR calibration in these two bands [12], [13], and despite the presence of atmospheric effects [14]–[16] is due to the normalization involved in its definition. The normalization reduces the effect of degradation of the satellite calibration from 10–30% for a single channel to 0–6% for the normalized index [12], [13]. The effects of the angular dependence of the surface bidirectional reflectance and of the atmospheric effects, is also reduced significantly in the normalized index [16]–[18]. The effect of scattering and absorption by atmospheric aerosol and gases (mainly water vapor) and by undetected clouds is reduced significantly in the compositing of the NDVI from several consecutive images, choosing a value that corresponds to the maximum vegetation index for each pixel [18]–[19].

Despite the inherent "resistance" of the vegetation index to calibration and atmospheric effects, any future advances in the quantitative application of the vegetation index to remote sensing of the biosphere and to studies of the biosphere–atmosphere interactions, would require further reduction of the atmospheric and sensor effects on the NDVI. This further reduction can be achieved in the EOS-MODIS era by several possible approaches:

1) Reduction of the effect of gaseous absorption by choosing narrow channels in atmospheric windows [20], [21], so that there will be no dependence of the NDVI on water vapor.
2) High spectral stability and calibration accuracy of the MODIS channels [20].
3) Development of methods for remote sensing of the atmospheric aerosol from satellite imagery [21]–[24] and application to atmospheric corrections of remotely sensed data [22], [25].
4) Redefinition of the NDVI so it will remain sensitive to variations in green vegetation, while being resistant to atmospheric effects.

The term "resistant to atmospheric effects" refers to significantly smaller variations in the value of ARVI for a given variation in the atmospheric opacity, than that of the NDVI.

Manuscript received September 26, 1991; revised November 1, 1991.

The authors are with the NASA/Goddard Space Flight Center, Greenbelt, MD 20771.

D. Tanré is on leave from Laboratoire d'Optique Atmospherique, Universite de Sciences et Techniques de Lille, Villeneuve d'Ascq, France.

IEEE Log Number 9105384.

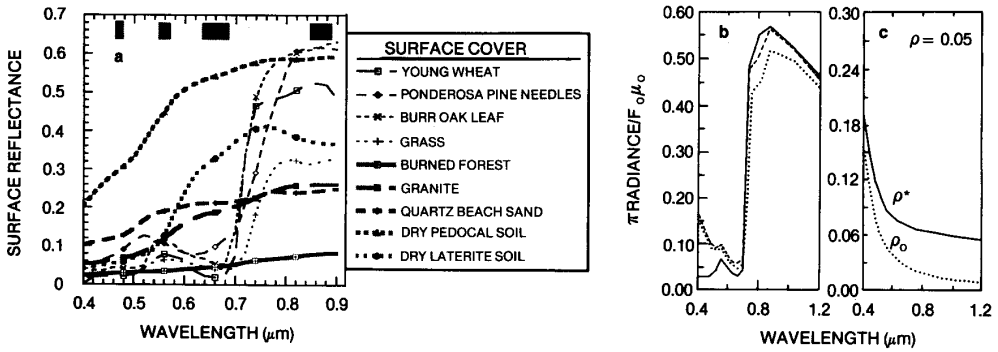

Fig. 1. (a) Surface reflectance spectra for several vegetation types, thin black lines, and several soil types, thick gray lines (data from Bowker *et al.* [4]), showing the relation between the reflectance in the blue band and the reflectance in the red band. The MODIS land channels in this spectral region are also shown (shaded areas). (b) Surface spectral reflectance for dense alfalfa — solid line [37] and the upward spectral normalized radiance for two atmospheric models with moderate aerosol loading (aerosol optical thickness of 0.25 at 0.56 μm) for low (dashed line) and high (dotted line) absorption, after Fraser and Kaufman [31]. Computations are performed for Angstrom exponent α=1.0. The effect of atmospheric scattering is strong for short wavelengths, and the effect of atmospheric absorption for longer wavelengths. (c) The normalized atmospheric path radiance ρ_o, and the total upward normalized radiance ρ^* for constant surface reflectance of $\rho = 0.05$ as a function of wavelength (after Kaufman, [25]).

The latest approach is the purpose of the present paper. It is envisioned that in the EOS era, remote sensing of vegetation will be performed by a combination of atmospheric correction for the well accounted for, molecular scattering and ozone absorption [18] followed by application of a vegetation index that is significantly less dependent on the atmospheric aerosol scattering. This approach is expected to reduce the atmospheric contamination so significantly, that for remote sensing of most of the globe no additional correction for the atmospheric effects on the vegetation index will be able to further reduce the errors. Detailed atmospheric correction for the aerosol effect will be still needed for highly contaminated atmospheric conditions such as arid and semiarid regions [23], [26], tropical regions during biomass burning [27], [28], and summertime in the eastern U.S. or Europe, contaminated by anthropogenic emissions [15], [29]. Note that atmospheric corrections will be still needed for other remote sensing applications, e.g., remote sensing of the bidirectional reflection of the surface, surface albedo, spectral classification, etc. [18].

In Section II the conceptual approach to the new vegetation index, ARVI, is developed. In Section III the resistance of the new vegetation index to atmospheric effects is demonstrated for several natural surface covers and compared to the original vegetation index. A sensitivity study of the ARVI is developed in Section IV, and optimization for remote sensing of soils and vegetation is given in Section V. Relation of the ARVI to other vegetation indexes are discussed in Section VI. Section VII concludes this paper.

II. Conceptual Approach to Atmospherically Resistant NDVI

The conceptual approach for the development of the atmospherically resistant NDVI is based on the spectral characteristics of vegetation and soils (Fig. 1(a)) and on the spectral characteristics of the atmospheric effect (Figs. 1(b) and (c)). The spectral upward radiance at the top of the atmosphere $L(\lambda)$ is related to the spectral surface reflectance $\rho(\lambda)$ by [30]:

$$L(\lambda) = L_o(\lambda) + \rho(\lambda)[F_d(\lambda)T(\lambda)/\pi]/[1 - s(\lambda)\rho(\lambda)] \quad (2)$$

where, $L_o(\lambda)$ is the atmospheric path radiance, due to solar radiation that was scattered by the atmosphere to the sensor without being reflected from the earth surface, $F_d(\lambda)$ is the spectral downward flux, $T(\lambda)$ is the total transmission of solar radiation reflected from the surface, through the atmosphere to the sensor, and $s(\lambda)$ is the backscattering coefficient of the upward radiation by the atmosphere. The coupling term $[1 - s(\lambda)\rho(\lambda)]$ is usually small [31] and for simplicity will be ignored in this discussion (the detailed computations in this paper, do account for it). The radiances $L(\lambda)$, $L_o(\lambda)$ are normalized to reflectance units and referred to as — normalized radiance:

$$\rho^*(\lambda) = \pi L(\lambda)/(F_o\mu_o), \rho_o(\lambda) = \pi L_o(\lambda)/(F_o\mu_o) \quad (3)$$

and the flux $F_d(\lambda)T(\lambda)$ is normalized by

$$f(\lambda) = F_d(\lambda)T(\lambda)/(F_o\mu_o) \quad (3')$$

where μ_o is the cosine of the solar zenith angle and F_o is the extraterrestrial solar flux. Therefore, (2) is reduced to:

$$\rho^*(\lambda) = \rho_o(\lambda) + \rho(\lambda)f(\lambda) \quad (4)$$

The atmospheric effect on the detected signal $\rho^*(\lambda)$ is composed from the normalized path radiance $\rho_o(\lambda)$ that increases the detected signal and from the transmission $f(\lambda)$ that decreases the detected signal. For low surface reflectance ($\rho < 0.1$), e.g., for all green vegetation and many soil types in the red channel, the net atmospheric effect is usually an increase in the detected signal. For higher surface reflectance ($\rho > 0.15$), e.g., for most surfaces in the near IR, the net effect is a mixed one. Increase or decrease of the signal, in this case, depends more on the characteristics of the atmospheric aerosol (e.g., the ratio of scattering to absorption) rather than their amount or total opacity [31]. As a result, the atmospheric effect on the red channel is much larger than on the near IR. Therefore, the effort to redefine the NDVI, to be more resistant to atmospheric

effects, is directed toward reduction of the effect on the red channel.

For MODIS, molecular scattering and ozone absorption take place mainly in atmospheric layers that are above the aerosol layer. Therefore, it is possible to correct the normalized radiances for molecular scattering and ozone absorption, thus reducing the normalized radiances observed from the satellite to just above the aerosol layer. We performed this correction assuming that the apparent reflectivity of the earth as observed from above the haze layer (and including the haze effect) is Lambertian. This simplification was found to introduce some errors when applied to radiances over the ocean [32], and methods for its correction were suggested [32]. In the rest of the text the normalized radiances are considered to be corrected for the molecular scattering and absorption.

In order to make the ARVI less dependent on variations of the atmospheric effect, it will be defined using, in addition to the red channel, the blue channel, in a self-correcting approach. Similar to (1), but written for the normalized radiance:

$$\text{ARVI} = (\rho^*_{\text{NIR}} - \rho^*_{\text{rb}})/(\rho^*_{\text{NIR}} + \rho^*_{\text{rb}}) \tag{5}$$

where

$$\rho^*_{\text{rb}} = \rho^*_{\text{r}} - \gamma(\rho^*_{\text{b}} - \rho^*_{\text{r}}) \tag{5'}$$

The subscripts r and b denote the red and the blue channels, respectively. Since the quantities ρ^*_{b}, ρ^*_{r} and ρ^*_{NIR} are already corrected for molecular scattering and gaseous absorption, the only contamination due to the atmosphere is from aerosol scattering and absorption (we do not discuss the effect of undetected clouds [19] in this content). The reason for the self-correcting characteristics of the new index, ARVI, can be explained, by comparing the red normalized radiance, ρ^*_{r}, used in the original NDVI, with the combined red–blue normalized radiance, ρ^*_{rb} that is resistant to the atmospheric effects. Substituting ρ^* from (4), and using the definition of ρ^*_{rb} 5′:

$$\rho^*_{\text{r}} = \rho_{o-\text{r}} + \rho_{\text{r}} f_{\text{r}} \tag{6}$$

$$\rho^*_{\text{rb}} = \rho_{o-\text{rb}} + \rho_{\text{r}} f_{\text{r}} + \gamma \Delta\rho_{\text{rb}} \tag{7}$$

where

$$\rho_{o-\text{rb}} = \rho_{o-\text{r}}(1+\gamma) - \gamma\rho_{o-\text{b}} \text{ and } \Delta\rho_{\text{rb}} = \rho_{\text{r}} f_{\text{r}} - \rho_{\text{b}} f_{\text{b}}$$

The main atmospheric effect in the new vegetation index, ARVI, is introduced through the normalized path radiance $\rho_{o-\text{rb}}$. Since the value of γ is not specified as yet, we can choose it so that $\rho_{o-\text{rb}}$ is minimal: $\rho_{o-\text{rb}} \ll \rho_{o-\text{r}}$ or even equal to zero. For a fixed aerosol model, we can choose γ to be:

$$\gamma = \rho_{o-\text{r}}/(\rho_{o-\text{b}} - \rho_{o-\text{r}}) \Rightarrow \rho_{o-\text{rb}} = 0 \tag{8}$$

But since the relative value of $\rho_{o-\text{r}}$ to $\rho_{o-\text{b}}$ depend on the aerosol characteristics, γ will depend on the aerosol type. Therefore, the degree of resistance of ARVI to atmospheric effects depends on the success in finding a single value of γ (or a simple scheme to compute γ) that reduces the atmospheric effect significantly on a global scale. In the next few paragraphs we shall discuss it further using the analytical expressions (5–8). In the rest of the paper we shall demonstrate that a single value of γ can reduce significantly the atmospheric effects and we shall optimize this value.

Measurements show that the aerosol radiative characteristics needed to describe the scattering phase function can be modeled by separating the different continental aerosol types into two types: dust storm aerosol and other aerosol types [33]. For large dust particles the aerosol optical thickness and the path radiance are wavelength independent. Therefore, $\rho_{o-\text{b}} \approx \rho_{o-\text{r}}$, resulting in $\gamma \to \infty$ in (8). As a result, the ARVI is not expected to be much better than the NDVI for large dust particles. But for other aerosol types the aerosol optical thickness, τ_a, is wavelength dependent $-\tau_a \approx C\lambda^{-\alpha}$, where α=1–2 [33–35] resulting in $\rho_{o-\text{b}} > \rho_{o-\text{r}}$. Therefore, it can be expected that a single value of γ will reduce the value of $\rho_{o-\text{rb}}$ significantly below the value of $\rho_{o-\text{r}}$.

The self-correction process described in (7), for a proper value of γ, reduces to a minimum the effect of the normalized path radiance $\rho_{o-\text{rb}}$ on the vegetation index. But it also involves the reflectance of the surface in the blue and the red bands, as well as atmospheric attenuation introduced in $\Delta\rho_{\text{rb}}$. For zero aerosol optical thickness, $\tau_a = 0$, $\Delta\rho_{\text{rb}}$ introduces a shift in the value of the ARVI relative to the corresponding value of the NDVI (see next section for examples), by replacing ρ_r with ρ_{rb}. For a nonzero τ_a, $\Delta\rho_{\text{rb}}$ introduces a small atmospheric effect that is not present in the NDVI of:

$$\delta\rho_{\text{rb}} = \gamma[\rho_{\text{b}}(1 - f_b) - \rho_{\text{r}}(1 - f_r)] \tag{9}$$

which, for example, for moderate atmospheric conditions over grass is $\delta\rho_{\text{rb}} = -0.007$. This atmospheric effect is accounted for, together with the residual atmospheric effect on the path radiance, in the computation of the optimum value of γ in Section V. For pure vegetation, the difference between the reflectance in the blue and the reflectance in the red is small (Fig. 1(a)). Therefore, the value of the difference $\Delta\rho_{\text{rb}}$ is small, and the corresponding atmospheric contamination is small. For soils, the difference is larger, and the contamination is expected to be larger.

This qualitative discussion describes the principle of the "atmospherically resistant" new vegetation index, ARVI. Quantitative simulations follows in the next sections.

III. Demonstration of the New Vegetation Index

In this section the resistance of the ARVI to atmospheric effects is compared with the atmospheric dependence of the original NDVI. The indexes are applied to three vegetation covers: grass [4], forest [36], and alfalfa [37], and two types of soils, [4] and [37], as a function of the fraction of the surface covered by the vegetation. The resultant reflectance is a weighted average of the soil and vegetation reflectance (for each vegetation and soil type) with the fraction of vegetation cover serving as the weighing factor. The simulation of the atmospheric effects is performed using the 5S radiative code [38] for the three spectral bands that compose the ARVI index: 0.47±0.01 μm, 0.66±0.025 μm, and 0.865±0.02 μm. Since atmospheric effects are slowly varying with the wavelength, the single value of the wavelength represents the average over

the spectral band. The 5S code, that was shown to be very accurate for low to moderate aerosol content [38], is applied to compute the normalized radiance detected by the satellite for three atmospheric aerosol models: continental aerosol with visibility of 25 km and 10 km, and maritime aerosol with visibility of 25 km. As mentioned in the previous section, before computing the vegetation index, the radiances were corrected for molecular scattering by subtracting the path radiance for $\tau_a = 0$ and dividing by $f(\lambda)$ for $\tau_a = 0$.

In Fig. 2, the vegetation indexes, ARVI and NDVI, are plotted for the three vegetation types as a function of the fraction of the surface covered by vegetation. The computations of ARVI are done for $\gamma = 1$, which will be shown later to be the optimum single value of γ in remote sensing applications. The indexes are plotted for the three atmospheric models as well as for an atmosphere without aerosol loading, where the vegetation indexes are computed directly from the actual surface reflectances. The differences in the values of the vegetation indexes between these models, shows the magnitude of the atmospheric effect. The original NDVI varies as a function of the atmospheric conditions by up to δNDVI = 0.2. The new index varies only within δARVI = 0.05. The atmospheric effect on the NDVI and its improvement by the ARVI index, are larger for densely vegetated surface than for bare soil.

IV. Sensitivity Study

The effect of the atmospheric aerosol on the NDVI is defined by the spectral dependence of the normalized atmospheric path radiance $\rho_o(\lambda)$ and transmission function $f(\lambda)$ (4). Its magnitude depends mainly on the ratio of the atmospheric path radiance to the surface reflectance. The spectral dependence of $\rho_o(\lambda)$ and $f(\lambda)$ are determined by the aerosol type, size and chemical composition. The magnitude of $\rho_o(\lambda)$ and $f(\lambda)$ is mainly determined by the aerosol content (or optical thickness) [25].

In order to simplify the computations in the sensitivity study, the atmospheric effect is described by simple analytical expressions for $\rho_o(\lambda)$ and $f(\lambda)$,

$$\rho_o(\lambda) = \omega_o(\lambda)\tau_a(\lambda)p(\theta,\lambda)/(4\mu_0\mu_v) \tag{10}$$

and

$$f(\lambda) = 1 - b(\lambda)\omega_o(\lambda)\tau_a(\lambda)(1/\mu_0 + 1/\mu_v) \tag{11}$$

where $\tau_a(\lambda)$ is the spectral aerosol optical thickness, $\omega_o(\lambda)$ is the aerosol single scattering albedo, $p(\theta,\lambda)$ the aerosol phase function and $b(\lambda)$ can be expressed by the asymmetry factor $g(\lambda)$ by: $b(\lambda) = (1 - g(\lambda))/2$ [38]. μ_0 and μ_v are, respectively, the cosines of the solar zenith angle θ_0 and the viewing zenith angle θ_v. Equations (10) and (11) are computed using a linearized single scattering approximation [31], [38].

The resistance of the ARVI to atmospheric effects depends on the surface type and on the radiative properties of the atmosphere. The sensitivity study is based on three types of natural surfaces: boreal forest [36], grass [4], and bare soil [37]. The surface reflectance in the three spectral bands are reported in Table I. For the atmospheric component, the type of aerosols is accounted for by a power law size distribution

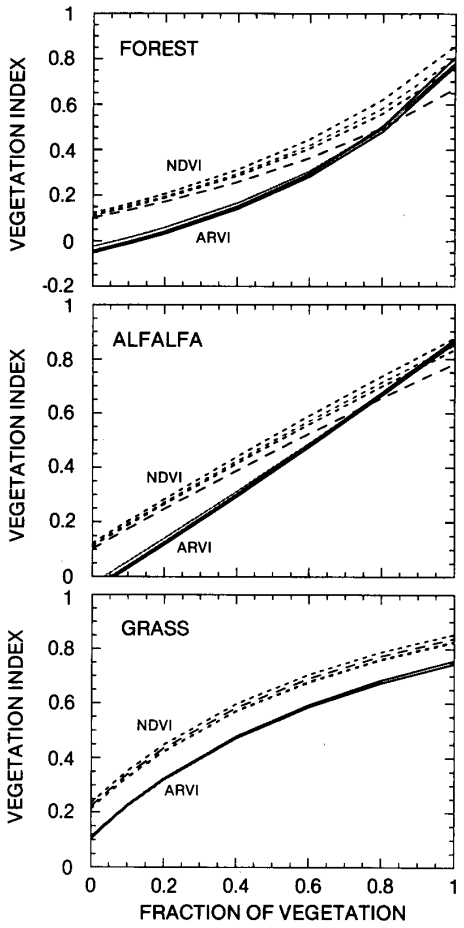

Fig. 2. The original vegetation index, NDVI (dashed lines) and the new vegetation index, ARVI (solids lines), as a function of the fraction of the surface covered by vegetation for forest, alfalfa, and grass. Computations were performed using the 5S radiative code [38], and surface reflectances were taken from Bowker *et al.* [4], Deering, [37], and Williams *et al.* [36]. Solar zenith angle is 60° and nadir view.

with an Angstrom exponent α [34] within the range $\alpha = 0-2$. $\alpha = 0$ corresponds to large particles such as the Saharan dust over arid regions [23], [26], $\alpha = 2$ corresponds to small particles such as smoke particles resulting from fires [28], [39]. Anthropogenic aerosol fall in between these values of α [35]. The radiative parameters: phase function, single scattering albedo, and asymmetry parameter are assumed to be spectrally independent and the only variable is the optical thickness, $\tau_a(\lambda)$, with a dependence $\tau_a(\lambda) = C\lambda^{-\alpha}$. In the application and optimization section (Sections II and V) the complete radiative 5S code of Tanré *et al.* [38] is used with the appropriate spectral radiative properties of several aerosol models. The similarity between the results of this section and the full radiative computations given in Section V, show that, as expected, the present simplifications do not alter substantially the results. Herein, the radiative parameters are taken from a continental aerosol model, $p(\theta,\lambda) = 0.20$, $\omega_o(\lambda) = 1.0$ and $g(\lambda) = 2/3$ [40] and standard or nominal

TABLE I
REFLECTANCES OF TYPICAL SURFACES IN THE THREE BANDS

Surface Cover	R_{blue}	R_{red}	R_{NIR}
Soil [37]	0.110	0.190	0.243
Grass [4]	0.012	0.052	0.660
Forest [36]	0.010	0.016	0.210

atmospheric conditions corresponding to $\alpha = 1.3$ (α was computed using the data of Shettle and Fenn [41]). The view and illumination angles are $\theta_0 = 60°$ and $\theta = 0°$.

The sensitivity of the ARVI to concentration of atmospheric aerosol can be expressed as a derivative, η,

$$\eta = \delta(\text{ARVI})/\delta\tau_a \tag{12}$$

The analytical expressions (10) and (11) allows us to compute η and to find the optimum value of γ (defined in (5)) for which the derivative, η, is minimum. The sensitivity of the optimum value to atmospheric and surface conditions is addressed in this section.

A. Sensitivity to Aerosol Size Distribution

For the three selected surfaces, the sensitivity of ARVI to atmospheric variation, $\eta = \delta(\text{ARVI})/\delta\tau_a$, is computed as a function of α for four values of γ: 0.0, 0.5, 1.0, and 2.0. γ = 0 is the value for which the ARVI is equal to the NDVI. The results are plotted as a function of the Angstrom exponent in Fig. 3.

The ARVI for bare soils (Fig. 3) has a weak sensitivity [$\eta \approx \pm 0.05$] to aerosol optical thickness. For the moderate values of soil reflectance (see Table I) it is less sensitive to the presence of a scattering layer because of compensation between the increase in the normalized path radiance, $\rho_o(\lambda)$, and the decrease in the normalized flux $f(\lambda)$ (in (4)) [18], [31]. For instance, a variation in the aerosol optical thickness of $\Delta\tau_a = 0.2$, results in an error of $\delta(\text{NDVI}) \approx 0.01$ in the NDVI. Use of ARVI results in a systematic improvement for γ = 0.5. For γ = 1.0 ARVI gives the same sensitivity [$\eta = 0.05$] as NDVI for nominal conditions (α = 1.30), e.g., continental aerosol, and better results for larger particles (α = 0.0). γ = 2.0 results in a large overcorrection for any value of α resulting in a sensitivity to the aerosol effect that is larger than for the original NDVI. For grass, due to the lower surface reflectance in the red channel, NDVI shows a larger sensitivity, around $\eta = -0.23$ and ARVI gives better results for any values of α and $\gamma \geq 0.5$. Forest, with even lower surface reflectance in the red band, presents the strongest sensitivity, $\eta \approx -0.75$ which corresponds to a large error in the NDVI of $\delta(\text{NDVI}) = 0.15$ for an aerosol optical thickness of 0.2. As for grass, ARVI provides for the forest better results for any value of α and $\gamma \geq 0.5$, with best results obtained for γ between 1.0 and 2.0.

These results confirm the importance of aerosol scattering effects on vegetation index for densely vegetated areas [18]. ARVI shows substantially less sensitivity to the aerosol content than NDVI. Except for bare soil, γ = 1.0 and γ = 2.0 reduces substantially the sensitivity of ARVI to atmospheric effects in respect to the sensitivity of the NDVI. For small particles ($\alpha > 1.5$) a high value of γ, γ = 2.0, may result in an overcorrection of the atmospheric effect, resulting in errors that are similar or even larger than the errors in the original NDVI ($\gamma = 0.0$). A value of γ of 1.0 seems more appropriate if information on the aerosol type is not available.

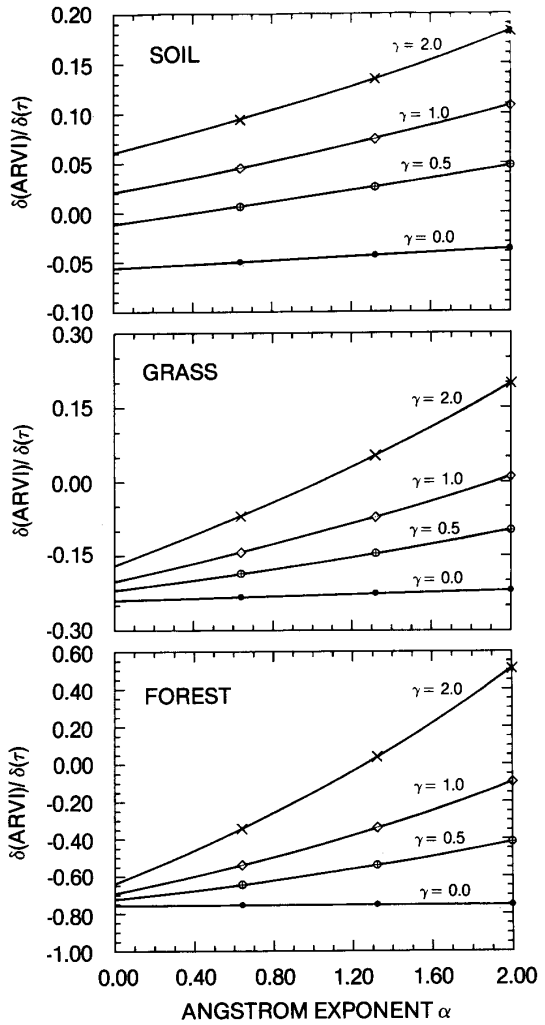

Fig. 3. Sensitivity of the new vegetation index, ARVI, to variations in the aerosol optical thickness τ_a: $\delta(\text{ARVI})/\delta\tau_a$, as a function of the Angstrom exponent α, for four values of γ: 0.0, 0.5, 1.0, and 2.0. γ = 0 is the value for which ARVI is equal to the NDVI. Results are given for soil, grass, and forest. The exponent α is used here to describe the aerosol type (α = 0 for large dust particles, α = 0.2 for maritime aerosol, α = 1.3 for continental aerosol, and α = 2 for smoke particles).

B. Relation Between γ, α, and Vegetation Fraction

In Fig. 4 we examine the sensitivity of the new vegetation index to variation in the fraction of vegetation cover (for grass) and in the Angstrom coefficient, α, for four values of γ. Contour lines of equal δ(ARVI) for $\tau_a = 0.1$ are plotted in the parameterization space with two dimensions: vegetation fraction and α, for four value of γ: 0 (no correction), 0.5, 1.0, and 2.0. This parameterization space covers all the basic

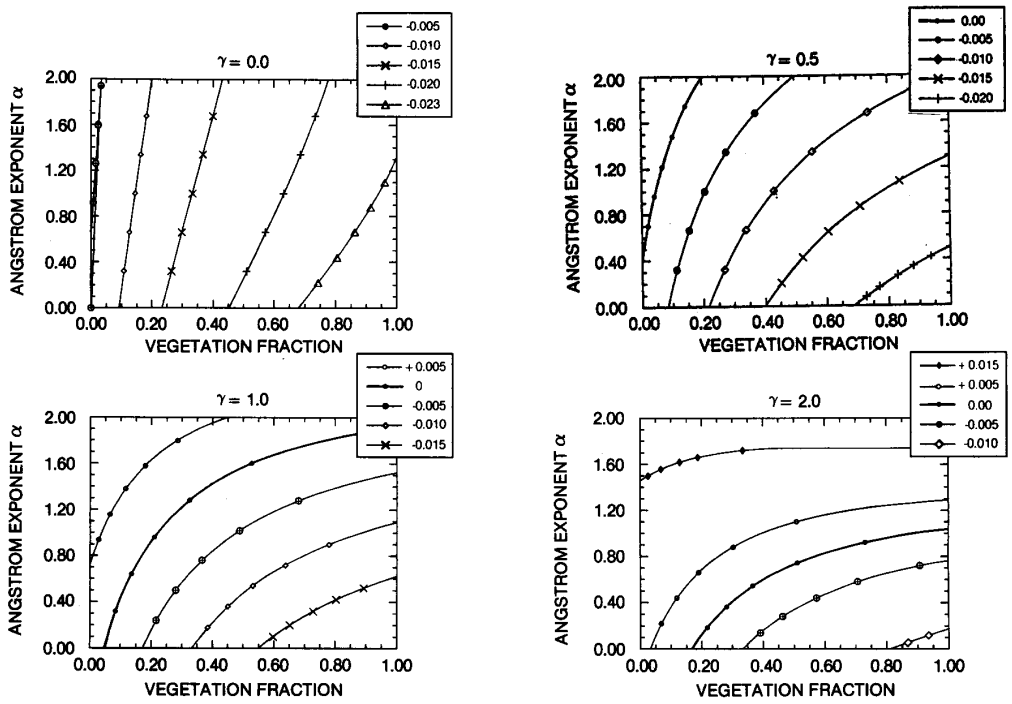

Fig. 4. Sensitivity of the new vegetation index, ARVI, to variation in the fraction of vegetation cover (for grass) and in the Angstrom coefficient, α. Contour lines of equal change in ARVI $-$ δ(ARVI) are plotted for $\tau_a = 0.1$ in the parameterization space with dimensions of the vegetation fraction and α. Results are given for four value of γ: 0.0 (no correction), 0.5, 1.0 (the optimum value), and 2.0. This parameterization space covers, in a simplified form, all the possible conditions of remote sensing, varying the surface properties by changing the vegetation cover and changing the size distribution, and the corresponding optical characteristics of the aerosol layer. Note that continental aerosol is characterized by $\alpha = 1.3$ and maritime aerosol by $\alpha = 0.2$.

conditions of remote sensing, varying the surface properties by changing the vegetation cover (though only for grass and one type of soil) and changing the size distribution, and the corresponding optical characteristics of the aerosol layer. Note that for $\gamma = 1.0$, the isoline that corresponds to zero error covers the "main grounds" in this parameterization space. It starts from low vegetation cover (e.g., arid to semiarid regions like the Sahel) and low value of α (e.g., dust, which is common in these regions [26]), and moves on to $\alpha = 1.3$–1.9 for vegetation fraction of 0.3–1.0, which is typical for vegetated regions [28], [35], [39], [42].

There are some exclusions to this remarkably suitable variation of the zero isoline for $\gamma = 1.0$. For larger values of vegetation cover (more than 60%), and for very humid conditions, which increase the particle size [35], [43] and decrease the value of α, the error in ARVI is large though still half as large as that for the NDVI ($\gamma = 0$). For very small vegetation cover, and for unknown aerosol particle size, a value of $\gamma = 0.5$ leads to better results, since for this value the isoline for zero error is very steep, thus resulting in a very good correction for any value of α.

As a conclusion, unless the aerosol model is know *a priori*, a single value of γ ($\gamma = 1.0$) should be adopted for minimizing the atmospheric effects. In specific conditions (e.g., the Sahel), a better value of γ ($\gamma = 1.0$) can be used (e.g., $\gamma = 0.5$). The single value of γ gives better results than the NDVI in any possible remote sensing condition.

C. Sensitivity to the Relation Between the Reflectance in the Blue and the Red Channel

In Fig. 5 the relation between the sensitivity of ARVI to the atmospheric effect and the values of the surface reflectance in the red (0.66±0.025 μm) and the blue (0.47 ±0.01 μm) channels are displayed. A scatter diagram of 40 different surface covers, including water, natural vegetation, agricultural crops, and soils (data are taken from [4]) is plotted. The average difference between the reflectances in the two channels is 0.08 for all the data, 0.04 for vegetation only, and 0.13 for soils only (see Table II). The dependence of an error in the ARVI $-$ δARVI resulting from a variation in the aerosol optical thickness of 0.2, on the reflectance in the blue and the red channels is shown by isolines for constant δARVI values. Computations of ARVI were performed for continental model ($\alpha = 1.3$) and for $\gamma = 1.0$ as a function of the surface reflectance in the blue and the red channels. The reflectance in the near IR is 0.4, the average value in Table II. The error in ARVI as a function of the surface reflectance in the two bands, for $\gamma = 1.0$ covers most of the surface types in Fig. 5, for a range of δARVI between -0.03 and $+0.01$. Therefore, ARVI should be suitable to be applied to other surface covers than those shown in Fig. 2.

V. Application and Optimization

The sensitivity, presented in the previous section, demon-

TABLE II
RELATION BETWEEN THE REFLECTANCE IN THE RED CHANNEL (0.66±0.025 μm) AND IN THE BLUE CHANNEL (0.47±0.01 μm)

surface/ property	reflectances [4] blue 0.47 μm	red 0.66 μm	NIR 0.86 μm	Ratio blue/red	difference	NDVI	ARVI
all surfaces	0.11±0.11	0.19±0.17	0.41±0.19	0.64±0.24	0.08±0.08	0.38±0.33	0.26±0.40
vegetation	0.06±0.04	0.10±0.07	0.45±0.18	0.71±0.25	0.04±0.05	0.63±0.25	0.55±0.32
soils	0.18±0.14	0.31±0.18	0.35±0.18	0.56±0.19	0.13±0.09	0.09±0.06	-0.08±0.08

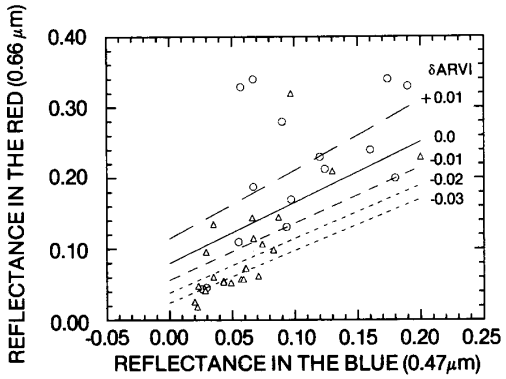

Fig. 5. The relation between the reflectance in the red (0.66±0.025 μm) and the blue (0.47±0.01 μm) bands for soils and water (o) and for vegetation (Δ) taken from Bowker *et al.* [4]. The sensitivity of the new vegetation index, ARVI, to the values of the reflectance in these two channels is also shown by isolines for constant δARVI values (lines) computed for a difference in the aerosol optical thickness of 0.2. Computations were performed for continental model (α = 1.3) and for γ = 1.0. The reflectance in the near IR was kept constant at 0.4.

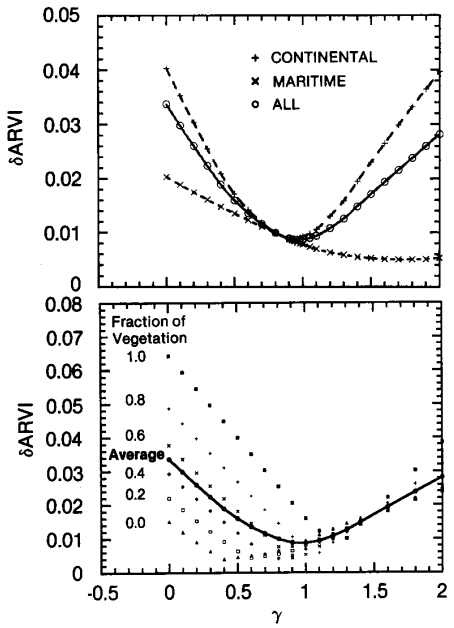

Fig. 6. The average difference, δARVI, between the value of ARVI for the continental and maritime atmospheric models and that for no atmospheric effect as a function of γ. The simulation is performed using the 5S code. (a) δARVI averaged over six values of the fraction of vegetation cover between 0 and 1, for the three vegetation types (forest, grass, and alfalfa). For the continental model the data were averaged for the two visibilities (10 and 25 km). The average between the three atmospheric models is also shown (o). (b) δARVI averaged over the three atmospheric models and the three vegetation covers, for several fractions of the vegetation cover.

strated the dependence of the optimum value of the parameter γ, introduced in the new vegetation index ((5)–(7)), on the surface and atmospheric properties. In this section, the simulation model (5S radiative code), used for the demonstration of the new vegetation index in Fig. 2, and described in Section III, is also used to compute the optimum value of γ for which the error (δARVI) in the derived index is minimum. The optimization is for several surface covers and atmospheric models. In Fig. 6 the average difference between the value of ARVI for the continental and maritime atmospheric models and that for the actual surface reflectance is plotted as a function of the value of γ. In Fig. 6(a) the difference is averaged over six values of the fraction of vegetation between 0 and 1, for the three vegetation types (forest, grass, and alfalfa), and for two soil types. For the continental model the results are averaged for the two visibilities (10 and 25 km). For Maritime aerosol only visibility of 25 km is used. The continental model represents moderate particle size with Angstrom exponent α = 1.3, and the maritime model represents large particles with α = 0.2. The average between the value of δARVI for the two continental models and the maritime model is also plotted. While for the continental model the optimum value of γ is around γ_{opt} = 0.9, for maritime model, with larger particle size (smaller value of α) the value is larger, γ_{opt} = 1.7. The plot that corresponds to the average of all these models shows minimum δARVI for γ_{opt} = 1.

In future application of the ARVI to MODIS data, an average value of γ_{opt} will be probably used to analyze most of MODIS images. In specific regions and seasons with defined vegetation and atmospheric properties, a special value may be applied. These possibilities are further explored in Fig. 6(b). As was already indicated in the sensitivity study of Section IV, a lower fraction of vegetation cover, corresponds to a lower optimum value γ_{opt}. Since the value of δARVI in Fig. 6(b) is asymmetrical around γ_{opt} = 1 the resulting range of variation in ARVI around γ_{opt} = 1 is small, between δARVI = 0.005 and 0.015. As a result, application of a constant value γ_{opt} = 1, even in cases where γ = 0.5 is more appropriate, will result in a small error δARVI for all surface covers (δARVI = 0.005 to 0.015) while a smaller value, γ = 0.5, which is better for soils, would result in large errors for pixels covered by vegetation (δARVI up to 0.06) that are located in the same image. Therefore, based on the present simulation it is recommended, that as a rule a single value of γ should be used. Unless the surface and atmospheric conditions are well known and require a substantially different value of γ (e.g., for

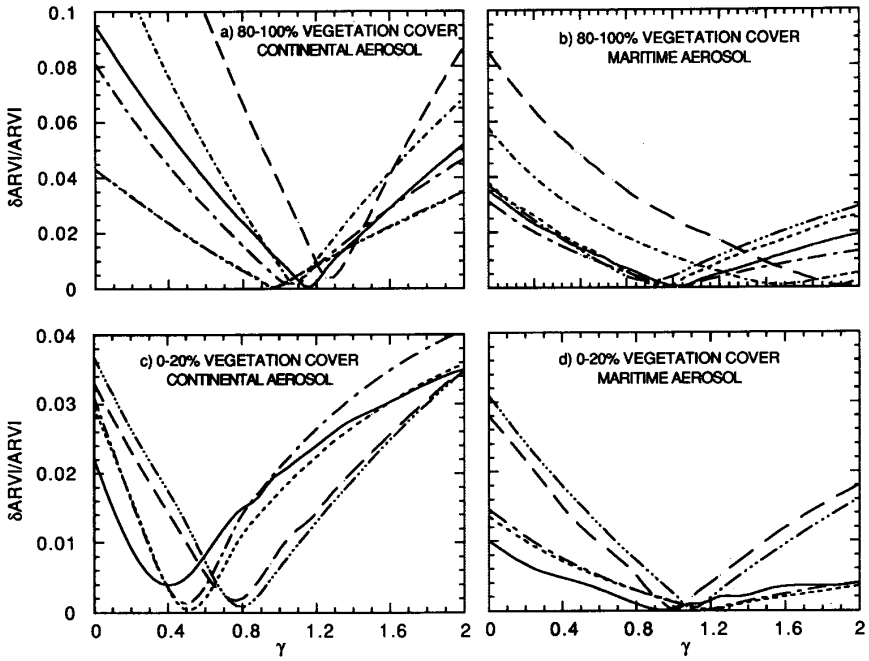

Fig. 7. Analysis of the dependence of the ratio δARVI/ΔARVI (ratio of noise to signal) on the value of γ for the two atmospheric models and for the humid vs. arid regions. The effect of the continental model ($\alpha = 1.3$) is shown in Figs. 7(a) and (c), and the effect of maritime model ($\alpha = 0.2$) in Figs. 7(b) and (d). Humid regions, are simulated by 80% and 100% vegetation cover (Figs. 7(a) and (b)) and arid conditions by 0 and 20% vegetation cover (Figs. 7(c) and (d)). The simulation is performed using the 5S code. For 7(a) and (b) the curves are: (——) — alfalfa, (– – –) — forest, (- - - - - -) — grass [4], (— - - -) — 80% alfalfa, (– - - -) — 80% forest, (— ... — ...—) — 80% grass. For 7(c) and (d) the curves are: (——) — soil [4], (– – –) — soil [37], (- - - - - -) — 20% alfalfa, (— - - -) — 20% forest, (— ... – ... —) — 20% grass.

vegetated area with large aerosol particles or for low vegetation fraction with small particle size), this value of $\gamma_{opt} = 1$ may be used.

The data in Fig. 6 can also be used to summarize the comparison between the residual dependence of ARVI and the NDVI on the atmosphere. For the selected value $\gamma = 1$, ARVI is in average four times less dependent on the atmospheric effects (δARVI four times smaller) than the NDVI (e.g., ARVI for $\gamma = 0.0$). For maritime atmosphere (or other larger aerosol particles), the improvement is only by a factor of two. For continental aerosol, the improvement is by more than factor of 4. Again, the improvement of the resistance of ARVI to atmospheric effects is much greater for vegetated regions than over arid regions (for $\gamma = 1$).

The ratio of δARVI/ΔARVI, shown in Fig. 7, is the ratio between the residual noise in the index (δARVI) due to the atmospheric effect and the signal that is sensitive to surface characteristics (ΔARVI). Here ΔARVI is defined as the difference between the value of ARVI for 100% vegetation cover and the value of ARVI for no vegetation. A detailed analysis of the dependence of this ratio on the value of γ for the two atmospheric models and for the humid vs. arid regions is shown in the figure. The effect of the continental aerosol is shown in Figs. 7(a) and (c), and the effect of maritime aerosol in Figs. 7 (b) and (d). Humid regions, are simulated by 80% and 100% vegetation cover (Figs. 7(a) and (b)) and arid conditions by 0 and 20% vegetation cover (Figs. 7(c) and (d)). The conclusions are very similar to the one drawn from the analysis of Figs. 4 and 6. The main advantage in the presentation of Fig. 7 is that we can see the individual errors for dry and humid regions for specific values of γ.

The consequences of using a single value of γ, $\gamma = 1.0$, for varying vegetation cover and atmospheric conditions, is shown in Fig. 8. The data are averaged for the three vegetation types and for the three atmospheric models, therefore, this figure represents the conditions for which the aerosol model and the type of vegetation that covers the surface are unknown. The value of γ for which the error δARVI is within 0.005 from the minimal value, is plotted in this figure. Due to the relatively small atmospheric effect over bare soil, the range of γ for which δARVI is within 0.005, is larger for low vegetation cover. Therefore, for the whole range of vegetation fraction, the additional error δARVI is always less than 0.005 for $\gamma = 1.0$.

VI. Relation to Other Vegetation Indexes

A change in the definition of the vegetation index in remote sensing applications may cause a discontinuity in global vegetation patterns. Therefore, it is important to check if it is possible to relate previous studies of the NDVI to vegetation properties derived from the new index — ARVI. The comparison in Fig. 2 shows that both indexes have a similar range for the five surface covers used in that figure. To expand the comparison between the two indexes for the

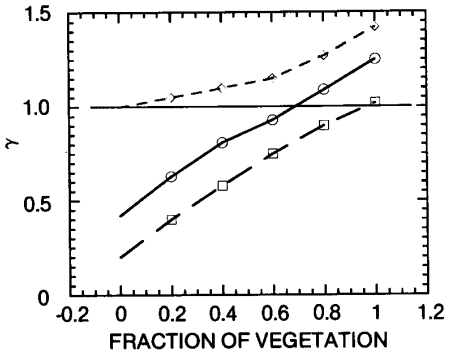

Fig. 8. The value of γ for which the error δARVI is within 0.005 from the minimal value, plotted as a function of the vegetation cover. The data are averaged for the three vegetation types and for the three atmospheric models. Therefore, this figure represents selection of γ in conditions for which the aerosol model is unknown, and the type of vegetation that covers the surface is also unknown. Solid line — γ values for minimum δARVI, dashed lines — γ values for δARVI 0.005 above the minimum.

pure surface reflectance, we plotted a scatter diagram of the values of ARVI as a function of the corresponding values of the NDVI. The vegetation indexes were computed for 44 surface covers from Bowker *et al.* [4] without atmospheric effects. The correlation coefficient between the two indexes is 0.98 and the relation is:

$$\text{ARVI} = -0.18 + 1.17 * \text{NDVI} \quad (13)$$

The similarity and high correlation between the two indexes should make the transfer from index to index relatively easy.

The concept of resistance to atmospheric variations in ARVI, which is based on the atmospheric information contained in the blue channel, can be applied also to other vegetation indexes than the NDVI. For example Huete [44] suggested to modify the definition of NDVI in order to make it less dependent on variation of soil properties, for partial vegetation cover. The resultant Soil Adjusted Vegetation Index (SAVI) is (eq. (4) in [44]) in present notations:

$$\text{SAVI} = (1 + C)(\rho^*_{\text{NIR}} - \rho^*_{\text{red}})/(\rho^*_{\text{NIR}} + \rho^*_{\text{red}} + C) \quad (14)$$

where C is a constant that is chosen as to minimize the soil effect ($C \approx 0.5$). Following the same analysis used in the derivation of (14) by Huete [44], the combined Soil Adjusted and Atmospherically Resistant Vegetation Index, SARVI, is obtained from (5) and (14):

$$\text{SARVI} = (1 + C)(\rho^*_{\text{NIR}} - \rho^*_{\text{rb}})/(\rho^*_{\text{NIR}} + \rho^*_{\text{rb}} + C) \quad (15)$$

The value of C in (15) is expected to be similar to that in (14).

VII. Conclusions

In order to reduce the dependence of the vegetation index NDVI on the atmospheric properties, a new atmospherically resistant vegetation index, ARVI, is proposed and developed to be used for remote sensing of vegetation from the Earth Observing System MODIS sensor. Same index can be used for remote sensing from the Landsat TM sensor, and the Earth Observing System HIRIS sensor. The index, defined by (5), replaces the red (0.66-μm) channel in the present NDVI with a combination of the red and the blue channels. This combination has self-correction properties for the atmospheric effect.

Simulations, for various atmospheric conditions, of the vegetation indices for Lambertian surfaces using the 5S radiative transfer code, show that ARVI is, on average, *four times less sensitive* to atmospheric effects than the NDVI. The improvement is much better for vegetated surfaces for which the atmospheric effect is larger than for soils. It is much better for moderate or small size of the aerosol particles (e.g., continental, urban, or smoke aerosol) than for large particle size (e.g., maritime aerosol or dust). Due to a nice coincidence, the same optimal value of the parameter γ ($\gamma = 1$) that defines the weighing of the blue band radiance in the ARVI definition, is found for vegetated areas with small to moderate aerosol particle size and for arid regions with large particle size. Therefore, a single value of γ may be used in all or most remote sensing applications.

In this study only results of simulation for a few AFGL atmospheric models [41] and a power law size distribution and Lambertian surfaces were reported, for one direction of illumination and observation. It is important to apply the new index to simulations using different characteristics of the surface, atmospheric aerosol and observation geometry. The index has to be tested against field data where the radiances are recorded over the same surface for varying atmospheric conditions. Experience with the analysis of ARVI in these conditions will verify how good ARVI is for global applications and whether a single value of the weighing γ should be used or γ should vary with surface and atmospheric conditions.

Acknowledgment

We would like to thank Shana Mattoo and Vincent Rose from ARC for part of the computations used in this work. The name of the new index, ARVI, was proposed by Brent Holben from NASA/GSFC. The concern of Jim Tucker, Brent Holben, Chris Justice, and others with atmospheric effects on the NDVI provided the inspiration for this research.

References

[1] C. O. Justice, J. G. R. Townshend, B. N. Holben, and C. J. Tucker, "Analysis of the phenology of global vegetation using meteorological satellite data," *Int. J. Remote Sensing*, vol. 6, pp. 1271–1318, 1985.

[2] C. J. Tucker, J. R. G. Townshend, and T. E. Goff, "African land cover classification using satellite data," *Science N. Y.*, vol. 227, pp. 369.3587–3594, 1985.

[3] C. J. Tucker, C. L. Vapraet, M. J. Sharman, and T. Van Ittersum, "Satellite remote sensing of total herbaceous biomass production in the Senegalese Sahel: 1980–1984," *Remote Sensing Environment*, vol. 17, pp. 233–249, 1985.

[4] D. E. Bowker, R. E. Davis, D. L. Myrick, K. Stacy, and W. T. Jones, "Spectral reflectances of natural targets for use in remote sensing studies," NASA Reference Publication 1139.

[5] P. J. Sellers, "Canopy reflectance photosynthesis and transpiration," *Int. J. Remote Sensing*, vol. 6, p. 1335, 1985.

[6] C. J. Tucker and P. J. Sellers, "Satellite remote sensing of primary productivity," *Int. J. Remote Sensing*, vol. 7, pp. 1395–1416, 1986.

[7] S. E. Nicholson, M. L. Davenport, and A. D. Malo, "A comparison of the vegetation response to rainfall in the Sahel and east Africa, using

NDVI from NOAA AVHRR," *Climate Change*, vol. 17, pp. 209–214, 1990.
[8] C. J. Tucker, I. Y. Fung, C. D. Keeling, and R. H. Gammon, "Relationship between atmospheric CO_2 variations and a satellite derived vegetation index," *Nature*, vol. 319, pp. 195–199, 1986.
[9] S. N. Goward, D. G. Dye, and C. J. Tucker, "North American vegetation patterns observed by NOAA-7 AVHRR," *Vegetation*, vol. 64, p. 3, 1985.
[10] S. D. Prince and C. J. Tucker, "Satellite remote sensing of rangelands in Botswana II: NOAA AVHRR and herbaceous vegetation," *Int. J. Remote Sensing*, vol. 7, pp. 1555–1570, 1986.
[11] J. R. G. Townsend and C. O. Justice, "Analysis of the dynamics of African vegetation using the NDVI," *Int. J. Remote Sensing*, vol. 7, pp. 1435–1446, 1986.
[12] B. N. Holben, Y. J. Kaufman, and J. D. Kendall, "NOAA-11 AVHRR visible and near-IR inflight calibration bands," *Int. J. Remote Sensing*, vol. 11, pp. 1511–1519, 1990.
[13] Y. J. Kaufman and B. N. Holben, "Calibration of the AVHRR visible and near-IR bands by atmospheric scattering, ocean glint and desert reflection," *Int. J. Remote Sensing*, in press, 1992.
[14] Y. J. Kaufman, "Atmospheric effect on remote sensing of surface reflectance," *SPIE*, vol. 475, pp. 20–33, 1984.
[15] R. S. Fraser, Y. J. Kaufman, and R. L. Mahoney, "Satellite measurements of aerosol mass and transport," *J. Atmos. Environ.*, vol. 18, pp. 2577–2584, 1984.
[16] B. N. Holben and R. S. Fraser, "Red and near IR sensor response to off-nadir viewing," *Int. J. Remote Sensing*, vol. 5, pp. 145–160, 1984.
[17] B. N. Holben, "Characteristics of maximum value composite images for temporal AVHRR data," *Int. J. Remote Sensing*, vol. 7, pp. 1417–1437, 1986.
[18] D. Tanré, B. N. Holben, and Y. J. Kaufman, "Atmospheric correction algorithm for NOAA-AVHRR products, theory and application," *IEEE Trans. Geosci. Remote Sensing*, vol. 30, pp. 000–000, 1992.
[19] Y. J. Kaufman, "The effect of subpixel clouds on remote sensing," *Int. J. Remote Sensing*, vol. 8, pp. 839–857, 1987.
[20] V. V. Salomonson, W. L. Barnes, P. W. Maymon, H. E. Montgomery, and H. Ostrow, "MODIS: Advanced facility instrument for studies of the earth as a system," *IEEE Trans. Geosci. Remote Sensing*, vol. 27, pp. 145–153, 1989.
[21] M. D. King, Y. J. Kaufman, P. Menzel, and D. Tanré, "Determination of cloud, aerosol, and water vapor properties from the Moderate Resolution Imaging Spectrometer (MODIS)," *IEEE Trans. Geosci. Remote Sensing*, vol. 30, pp. 2–27, 1992.
[22] Y. J. Kaufman and C. Sendra, "Algorithm for automatic atmospheric corrections to visible and near-IR satellite imagery," *Int. J. Remote Sensing*, vol. 9, pp. 1357–1381, 1988.
[23] D. Tanré, P. Y. Deschamps, C. Devaux, and M. Herman, "Estimation of Saharan aerosol optical thickness from blurring effects in Thematic Mapper data," *J. Geophys. Res.*, vol. 93, pp. 15955–15964, 1988.
[24] Y. J. Kaufman, R. S. Fraser, and R. A. Ferrare, "Satellite remote sensing of large scale air pollution - method," *J. Geophys. Res.*, vol. 95, pp. 9895–9909, 1990.
[25] Y. J. Kaufman, "The atmospheric effect on remote sensing and its correction," Chapter 9 in *Optical Remote Sensing, Technology and Application* G. Asrar, Ed. New York: Wiley, 1989.
[26] B. N. Holben, T. F. Eck, and R. S. Fraser, "Temporal and spatial variability of aerosol optical depth in the Sahel region in relation to vegetation remote sensing," *Int. J. Remote Sensing*, vol. 12, pp. 1147–1163, 1991.
[27] Y. J. Kaufman, C. J. Tucker, and I. Fung, "Remote sensing of biomass burning in the tropics," *J. Geophys. Res.*, vol. 95, pp. 9927–9939, 1990.
[28] Y. J. Kaufman, A. Setzer, D. Ward, D. Tanré, B. N. Holben, P. Menzel, M. C. Pereira, and R. Rasmussen, "Biomass Burning Airborne and Spaceborne Experiment in the Amazonas (BASE-A)," *J. Geophys. Res.*, in press, 1992.
[29] J. T. Peterson, E. C. Flowers, G. J. Berri, C. L. Reynolds, and J. H. Rudisil, "Atmospheric turbidity over central north Carolina," *J. Appl. Meteorol.*, vol. 20, pp. 229–241, 1981.
[30] S. Chandrasekhar, *Radiative Transfer*. New York: Dover, 1960.
[31] R. S. Fraser and Y. J. Kaufman, "The relative importance of scattering and absorption in remote sensing," *IEEE Trans. Geosci. Remote Sensing*, vol. 23, pp. 625–633, 1985.
[32] Deschamps, M. Herman and D. Tanré, "Modeling of the atmospheric effect and its application to the remote sensing of ocean color," *Appl. Opt.*, vol. 23, pp. 3751–3758, 1983.
[33] Y. J. Kaufman, "Measurements of the aerosol optical thickness and the path radiance — implications on aerosol remote sensing and atmospheric corrections," submitted for publication, *J. Geophys. Res.*, 1992.
[34] C. E. Junge, *Air Chemistry and Radiochemistry*. New York: Academic Press, 1963.
[35] Y. J. Kaufman and R. S. Fraser, "Light extinction by aerosols during summer air pollution," *J. Appl. Meteorol.*, vol. 22, pp. 1694–1706, 1983.
[36] D. Williams and C. L. Walthcell, "Helicopter based multispectral data collection over the northern experimental forest: Preliminary results from the 1989 field season," in *Proc. IGARSS 90*. New York: IEEE, 1990, pp. 875–878.
[37] D. W. Deering, "Field measurements of bidirectional reflection," Chapter 2 in *Optical Remote Sensing, Technology and Application*, G. Asrar, Ed. New York: Wiley, 1989.
[38] D. Tanré, C. Deroo, P. Duhaut, M. Herman, J. J. Morcrette, J. Perbos, and P. Y. Deschamps, "Description of a computer code to simulate the satellite signal in the solar spectrum: 5S code," *Int. J. Remote Sensing*, vol. 11, pp. 659–668, 1990.
[39] B. N. Holben, Y. J. Kaufman, A. Setzer, D. Tanré, and D. E. Ward, "Optical properties of aerosol from biomass burning in the tropics, BASE-A," in *Global Biomass Burning*. Cambridge, MA: MIT Press, 1991, pp. 403–411.
[40] R. A. McClathchey, R. W. Fenn, J. E. A. Selby, F. E. Volz, and J. S. Garing, "Optical properties of the atmosphere," AFCRL 72-0497, AD 75075, 1972.
[41] E. P. Shettle and R. W. Fenn, "Models for the aerosol of the lower atmosphere and the effect of humidity variations on their optical properties," AFGL-TR 790214, Opt. Phys. Div., Air Force Geophysics Laboratory, Hanscom AFB MA, 1979.
[42] K. T. Whitby, "The physical characteristics of sulfur aerosols," *Atmos. Environ.*, vol. 12, pp. 135–159, 1978.
[43] G. Hanël, "An attempt to intercept the humidity dependencies of the aerosol extinction and scattering coefficient," *Atmos. Environ.*, vol. 15, pp. 403–406, 1981.
[44] A. R. Huete, "A soil-adjusted vegetation index (SAVI)," *Remote Sensing Environment*, vol. 25, pp. 295–309, 1988.

Yoram J. Kaufman, for a photograph and biography, please see page 222 of this issue of the TRANSACTIONS.

Didier Tanré, for a photograph and biography, please see page 222 of this issue of the TRANSACTIONS.